On the period distribution of cluster RR Lyrae stars to constrain their helium content: the case of ω Centauri

M. Marconi[1], G. Bono[2,3,4], F. Caputo[3], A. M. Piersimoni[5], A., Pietrinferni[5], R., F. Stellingwerf[6]

ABSTRACT

We present new sets of nonlinear, time-dependent convective hydrodynamical models of RR Lyrae stars assuming two metal (Z=0.0005, Z=0.001) and three helium abundances (Y=0.24, 0.30, 0.38). For each chemical composition we constructed a grid of fundamental (FU) and first overtone (FO) models covering a broad range of stellar masses and luminosities. To constrain the impact of the helium content on RR Lyrae properties, we adopted two observables –period distribution, luminosity amplitudes– that are independent of distance and reddening. The current predictions confirm that the helium content has a marginal effect on the pulsation properties. The key parameter causing the difference between canonical and He-enhanced observables is the luminosity. We compared current predictions with the sample of 189 RR Lyrae stars in ω Cen and we found that the period range of He-enhanced models is systematically longer than observed. These findings apply to metal-poor and metal-intermediate He-enhanced models. To further constrain the impact of He-enhanced structures on the period distribution we also computed a series of synthetic HB models and we found that the predicted period distribution, based on a Gaussian sampling in mass, agrees quite well with observations. This applies not only to the minimum fundamentalized period of RR Lyrae stars (0.39 vs 0.34 day), but also to the fraction of

[1]INAF-Osservatorio astronomico di Capodimonte, Via Moiariello 16, 80131 Napoli, Italy; marcella.marconi@oacn.inaf.it

[2]Dipartimento di Fisica - Università di Roma Tor Vergata, Via della Ricerca Scientifica 1; giuseppe.bono@roma2.infn.it

[3]INAF-Osservatorio Astronomico di Roma, Via Frascati 33, 00040 Monte Porzio Catone, Italy; caputo@oa-roma.inaf.it

[4]European Southern Observatory, Karl-Schwarzschild-Str. 2, 85748 Garching bei Munchen, Germany

[5]INAF-Osservatorio Astronomico di Collurania, Via M. Maggini, Teramo, Italy; piersimoni@oa-teramo.inaf.it, adriano@oa-teramo.inaf.it

[6]Stellingwerf Consulting, 11033 Mathis Mtn Rd SE, 35803 Huntsville, AL USA; rfs@swcp.com

Type II Cepheids (2% vs 3%). We also computed a series of synthetic HB models assuming a mixed HB population in which the 80% is made of canonical HB structures, while the 20% is made of He-enhanced (Y=0.30) HB structures. We found that the fraction of Type II Cepheids predicted by these models is almost a factor of two larger than observed (5% vs 3%). This indicates that the fraction of He-enhanced structures in ω Cen cannot be larger than 20%.

Subject headings: globular clusters: individual (NGC 5139) — stars: abundances — stars: evolution — stars: horizontal-branch — stars: oscillations — stars: variables: RR Lyrae

1. Introduction

The stellar content of globular clusters (GCs) considered an optimal realization of a simple stellar population, since they are coeval and chemically homogeneous stellar systems, has been questioned. The spectroscopic evidence of star-to-star variations in the abundance of C, N and Na as well as of Al and O in many cluster Red Giant (RG) stars dates back to forty years ago (Osborn 1971). Moreover, the molecular band-strengths of CN and CH seem to be anti-correlated (Smith 1987; Kraft 1994) and anti-correlations between O–Na and Mg–Al have been observed in evolved (RG, Horizontal Branch [HB]), and in unevolved (Main Sequence [MS]) stars of all the GCs investigated with high-resolution spectra (Pilachowski, Sneden & Wallerstein 1983; Gratton, Sneden & Carretta 2004).

More recently, accurate and deep Hubble Space Telescope optical photometry disclosed the presence of multiple stellar populations in several massive GCs. Together with the most massive Galactic GC ω Cen (Anderson 2002; Bedin et al. 2004) multiple stellar sequences have been detected in GCs covering a broad range of metal content: NGC 2808 (Piotto et al. 2007), M54 (Siegel et al. 2007), NGC 1851 (Calamida et al. 2007; Milone et al. 2008) and 47 Tuc (Di Criscienzo et al. 2010; Nataf et al. 2011). Some of these multiple sequences (ω Cen, NGC 2808, NGC 1851) might be explained either with a He-enhanced(Norris 2004; Lee et al. 2005; D'Antona & Caloi 2008; Piotto et al. 2007), or with a CNO-enhanced (Calamida et al. 2007; Cassisi et al. 2008) sub-population. However, no general consensus has been reached concerning the physical mechanisms, the evolutionary history and the fraction of these stellar components (Bergbusch & Stetson 2009).

The possible occurrence of He-enriched stars in GCs was suggested to explain not only the presence of multiple unevolved sequences, but also the presence of extended blue HB tails (D'Antona & Caloi 2008, and references therein). Evolutionary prescriptions indicate

that He-enriched structures, at fixed metallicity and cluster age, have a smaller turn-off mass when compared with structures constructed by assuming a canonical He content. Therefore, a He-enriched sub-population, for a fixed mass loss rate, is characterized by smaller envelope masses and will *mainly* populate the hot and the extreme region of the HB (Bono 2010). Therefore, the presence of He-enriched sub-population(s) in GCs alleviates the heavy assumption of strong stochastic changes in the mass-loss rate along the RGB, required by the canonical scenario to populate the entire HB.

In this context ω Cen plays a key role, since it is a massive GC (Lee et al. 2009b) in which have been identified several MS and sub-giant branches (Bellini et al. 2010, and references therein). Low-resolution spectra indicate that the bluest MS is more metal-rich than the redder ones, thus further supporting the evidence that it could be He-enhanced (Norris 2004; Piotto et al. 2005). However, Castellani et al. (2007) using star count ratio of HB and RG stars suggested that a significant fraction of Extreme HB (EHB) stars in ω Cen might be aftermath of the *hot helium flashers* scenario[1]. By using a broad range of synthetic color-magnitude diagrams (CMDs) Cassisi et al. (2009) found that EHB stars ($Te \geq 30,000$ K) in ω Cen should be a mix of He-enhanced, *hot helium flashers* and canonical HB stars. In a spectroscopic investigation of ω Cen EHB stars, Moehler et al. (2010) found that roughly the 30% are He-poor, while the 70% have either solar or super-solar He abundances. Note that the carbon-rich stars are also He-rich stars, thus further supporting the evidence that a fraction of these stars is the progeny of the *hot helium flashers* scenario.

In a recent evolutionary investigation (D'Antona, Caloi & Ventura 2010) suggest that very high He abundances (Y=0.80) could be required to explain ω Cen EHB stars and that warm ($logT_e$<10,000 K, see their Fig. 2) HB stars might have He abundances ranging from the canonical to significantly higher He abundances. However, Sollima et al. (2006) using high-resolution spectra of 74 RR Lyrae stars in ω Cen found that their metallicity distribution agrees quite well with the metallicity distribution of RG stars (Calamida et al. 2009). Moreover, the distribution in the CMD of metal-intermediate RR Lyrae stars agrees quite well with the predicted metal-intermediate Zero-Age Horizontal Branch (ZAHB) based on HB models constructed assuming a canonical He content. The quoted authors pointed out that if the blue MS is made of He-enhanced, metal-intermediate MS stars, and if these

---

[1]Evolutionary models indicate that HB structures which ignite He along the white dwarf cooling sequence (*hot helium flashers*) experience a significant mixing (Miller Bertolami et al. 2008; Brown et al. 2010) between the core (He and carbon-rich) and the envelope (hydrogen rich). The structures experiencing this flash-mixing phenomenon show an increase in the surface abundance of carbon ranging from 1% to 5% and an increase in He content. This is a crucial observable, since the progeny of the He-enriched scenario is not supposed to be carbon-enriched.

structures are the progenitors of the EHB stars, then ω Cen should simultaneously host two metal-intermediate stellar populations with two different He contents.

In this investigation we address the helium content of ω Cen RR Lyrae using their period distribution and luminosity amplitude.

2. The theoretical framework

The new pulsation RR Lyrae models have been computed by using the hydrodynamical code developed by Stellingwerf (1982) and updated by Bono & Stellingwerf (1994); Bono, Marconi, & Stellingwerf (1999, see also Smolec & Moskalik (2010) for a similar approach). The physical assumptions adopted to compute these models will be described in Marconi et al. (2011, in preparation). We adopted the OPAL radiative opacities released in 2005 by (Iglesias & Rogers 1996, http://www-phys.llnl.gov/Research/OPAL/opal.html) and the molecular opacities by Alexander & Ferguson (1994). To constrain the pulsation properties of RR Lyrae stars in ω Cen, we adopted two metal abundances similar to the two observed peaks in the RR Lyrae metallicity distribution (Sollima et al. 2006), namely Z=0.0005 and Z=0.001. For each metal content we adopted three He contents to constrain the dependence of the pulsation properties of RR Lyrae stars on this crucial parameter. For each fixed chemical composition the stellar mass of RR Lyrae stars was fixed by using the evolutionary prescription for α-enhanced structures provided by Pietrinferni et al. (2006) and available on the BASTI database[2]. Note that for each fixed metal content the mass of the He-enhanced models was estimated assuming the same cluster age (13 Gyr). Together with the luminosity predicted by evolutionary models we often adopted a brighter luminosity level to account for the possible occurrence of evolved RR Lyrae stars. The input of the different sets of He-enhanced models are listed in Table 1, where columns from 1 to 4 give the metal and the He abundance, the stellar mass and the luminosity.

For each fixed chemical composition, mass value and luminosity level, we investigated the limit cycle behavior of both fundamental (FU) and first overtone (FO) pulsators by covering a wide range of effective temperatures. For each model the pulsation equations were integrated in time till the radial motions approached their limit cycle stability. This means that we can provide robust constraints not only on the topology of the instability strip (IS), but also on the pulsation amplitudes of He-enhanced models. The top and the

---

[2]http://albione.oa-teramo.inaf.it/

Table 1. Intrinsic stellar parameters adopted to compute canonical and He-enriched pulsation models.

Z[a]	Y[a]	$M/M_\odot$[b]	$\log L/L_\odot$[c]
0.0004	0.24[c]	0.70	1.6, 1.7, 1.8
0.0005	0.35	0.65	1.85, 1.95
	0.40	0.60	1.9
0.001	0.24[c]	0.65	1.5, 1.6, 1.7, 1.9
	0.30	0.60, 0.65	1.8, 1.9, 2.0
	0.38	0.60, 0.65	1.8, 1.9, 2.0

[a]Metal (Z) and helium (Y) abundance by mass.

[b]Stellar mass (solar units).

[c]ogarithmic luminosity (solar units).

[d]Canonical RR Lyrae pulsation models computed by Bono et al. (2003); Di Criscienzo, Marconi & Caputo (2004). The difference in metal content between the canonical and the He-enhanced models has a minimal impact on the pulsation properties and they are treated together.
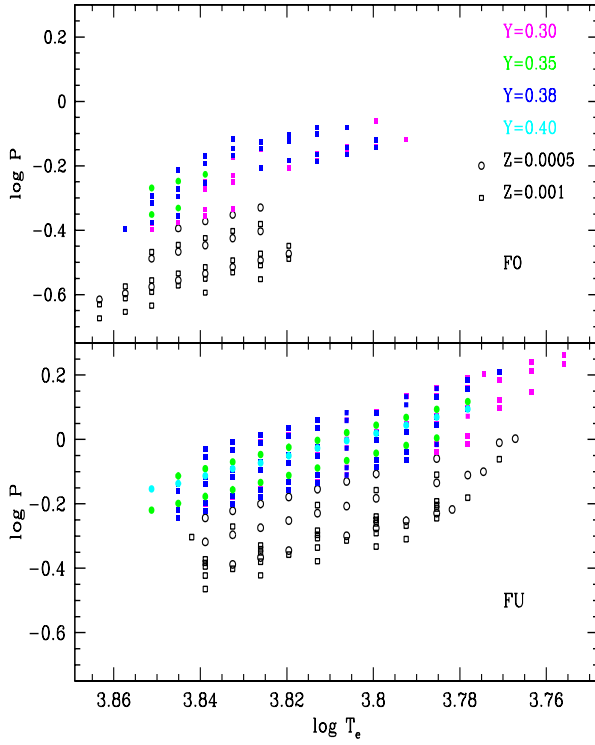
Fig. 1.— Top – Period distribution of metal-poor (Z=0.0005, open circles) and metal-intermediate (Z-0.001, squares) first overtone RR Lyrae models. The models with canonical He content are plotted as empty symbols, while the He-enhanced ones with filled symbols and different colors (see labels). Bottom – Same as the top, but for the fundamental RR Lyrae models.

bottom panel of Fig. 1 show the period distribution of canonical[3] (empty symbols) and He-enhanced (filled symbols) models. The circles and the squares display metal-poor and metal-intermediate RR Lyrae models.

A glance at the data plotted in Fig. 1, indicate that RR Lyrae models with a He-enhanced composition show periods that are systematically longer than the canonical ones. The difference is mainly caused by evolutionary effects. The top (canonical), the middle (He-enhanced, Y=0.30) and the bottom (He-enhanced, Y=0.38) panel of Fig. 2 show together with the modal stability of FU (solid vertical lines) and FO (dotted vertical lines) RR Lyrae stars the predicted ZAHBs (dashed line) and selected HB evolutionary models. On the basis of the evolutionary predictions plotted in this figure we can identify two different regimes.

HB structures evolving inside the instability strip –
The HB structures with a ZAHB location inside the IS and evolving during their central He-burning phases inside the RR Lyrae IS show, at fixed cluster age (13 Gyr) and metal content (Z=0.001), similar mass values when moving from a canonical (Y=0.24, top panel of Fig. 2) He content to a moderately He-enhanced (Y=0.30, middle panel of Fig. 2) abundance. The comparison cannot be extended to the more He-enhanced models (Y=0.38, bottom panel of Fig. 2), since the predicted ZAHB for these models minimally intersect the predicted RR Lyrae IS. The mass of the progenitors decreases from 0.80 to $0.70 M_\odot$ and to $0.62 M_\odot$ when moving from the lowest to the highest He content. The typical masses populating the IS of the canonical models range from ~ 0.64 to $\sim 0.69 M_\odot$, and the typical luminosity is $\log L/L_\odot \approx 1.70$. For moderately He-enhanced models the masses range from ~ 0.64 to $\sim 0.70 M_\odot$, and the typical luminosity is $\log L/L_\odot \sim 1.80$. Evolutionary prescriptions concerning moderately He-enhanced models (Y=0.30) indicate that HB structures evolving inside the IS are a mix between structures evolving from the blue to the red and also in the opposite direction. This effect is mainly caused by the fact that an increase in He-content causes an extension of the excursion toward hotter effective temperatures that these structures perform during their off-ZAHB evolution (see the bottom panel of Fig. 2; Sweigart & Gross 1976; Sweigart & Catelan 1998; Fig. 2 in D'Antona et al. 2010).

HB structures evolving across the instability strip –
The HB structures with lower total masses attain their location along the ZAHB toward effective temperatures hotter than RR Lyrae IS. During their off-ZAHB evolution they cross the IS at luminosities systematically brighter than typical RR Lyrae stars. For a hot HB

---

[3]The reader interested in a detailed discussion concerning the canonical RR Lyrae models is referred to Bono et al. (2003); Di Criscienzo, Marconi & Caputo (2004)
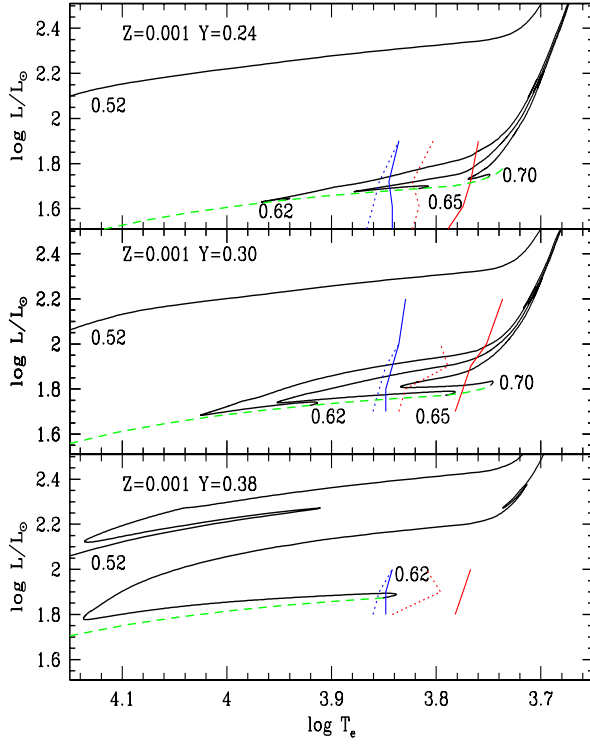
Fig. 2.— Top – Predicted RR Lyrae instability strip at fixed metal content (Z=0.001) based on canonical pulsation models. The solid and the dotted vertical lines display the instability strip for fundamental and first overtone RR Lyrae. The almost horizontal dashed line shows the predicted Zero-Age Horizontal Branch, while the solid lines selected HB evolutionary models (BASTI database) of different stellar masses. Middle – Same as the top, but for moderately He-enhanced models (Y=0.30). Bottom – Same as the top, but for He-enhanced models (Y=0.38).

structure of 0.52 M$_\odot$ the luminosity at the center of the IS ($\log T_{eff}$=3.83) is $\approx$2.30 for the Y=0.24 and Y=0.30 models and becomes 2.40 for the Y=0.38 models, while the period changes from P$\sim$2.0 to P$\sim$2.4 day. For a warm HB structure with a stellar mass of 0.62 M$_\odot$ the luminosity is $\log L/L_\odot \approx$1.76 for Y=0.24, $\approx$1.91 for Y=0.30 and $\approx$2.17 for Y=0.38, while the period increases by more than a factor of two: P$\sim$0.61, P$\sim$0.83 and P$\sim$1.36 day respectively. The main evolutionary consequence of the presence of He-enhanced models is that we can have HB structures with similar masses either evolving inside the IS or crossing the IS that are from 0.1 to $\sim$0.4 dex more luminous than the canonical ones. The main outcome of the quoted differences is to produce RR Lyrae stars with pulsation periods that are systematically longer than the canonical ones.

The above findings concerning the increase in the period of RR Lyrae stars supports the simulations provided by Sweigart & Catelan (1998) using He-enhanced models. The quoted authors investigated three different noncanonical scenarios to explain the tilted HB of two metal-rich GCs (NGC 6388, NGC 6441). They also investigated the impact on the period distribution of RR Lyrae and found that the increase in He causes a systematic increase in the luminosity, and in turn in the period of RR Lyrae stars (see their Fig. 3).

Two evolutionary effects are noteworthy concerning He-enhanced HB models. *Mass loss–* He-enhanced models (Cassisi et al. 2009; Di Cris] Criscienzo et al. 2010) alleviate the requirement of strong changes in the mass loss rate along the RGB. Current predictions also indicate that the mass loss rate of RG stars is independent of their He content. This means that if we assume multiple populations with different He-contents the ZAHB from the red HB to the EHB will be *naturally* populated with structures of different total mass. *Lifetime–* Evolutionary prescriptions indicate that the central He-burning lifetime of He-enriched structures is longer than for canonical HB (Cassisi et al. 2009; D'Antona, Caloi & Ventura 2010). The difference with the most He-enriched models ranges from 10% for red HB stars to 30% for EHB stars (logTe$\approx$4.3). The increase in the lifetime is caused by the fact that they are fainter, since the He-core mass of He-enhanced models is slightly smaller than the canonical ones. In these structures, the H-shell plays a marginal role, since the envelope mass is quite small. The HB region in which the H-shell becomes relevant in the energy budget is for effective temperatures cooler than logTe$\approx$4, and indeed in this region He-enhanced structures are brighter than canonical ones. However, the He-burning lifetime of He-enhanced models is longer over the entire temperature range. The difference is smaller and appears counter-intuitive, since the former structures are, at fixed effective temperature, brighter than the latter ones. The increase in the He-burning lifetime is mainly caused by the fact that the hydrogen-burning shell in the He-enriched structures is more efficient, due to the increase in the mean molecular weight (see Fig. 6 in Bono 2010). This means that the moderately He-enhanced sub-population is expected to populate the entire HB.

3.   Comparison with observations

To constrain the He content of RR Lyrae stars in ω Cen we adopted the period distribution. The reasons to use this observable are threefold. i)– ω Cen hosts a sizable sample of RR Lyrae stars (189: 100 RRc, 89 RRab Kaluzny et al. 2004; Weldrake, Sackett, & Bridges 2007). ii)– The distance modulus of ω Cen was fixed using the K-band Period-Luminosity relation of RR Lyrae stars (Del Principe et al. 2006) and with the tip of the RG branch (Bono et al. 2008). However, different authors are still adopting distance moduli that differ by more than 0.3 dex (Cassisi et al. 2009; D'Antona, Caloi & Ventura 2010). The period distribution is distance and reddening independent. iii)– The census of bright variables in this cluster is complete (Kaluzny et al. 2004; Weldrake, Sackett, & Bridges 2007).

Fig. 3 shows the period distribution of RR Lyrae stars in ω Cen using the sample adopted by Del Principe et al. (2006). The period distribution was smoothed using a Gaussian kernel (for more details see Di Cecco et al. 2010). The comparison between theory and observations brings forward interesting results: i)– The period range covered by He-enhanced models is systematically longer than observed. The discrepancy becomes even more clear if we account for the fact that variables with periods longer than $\approx$0.9 day are classified as Type II Cepheids[4]. ii)– The He-enhanced models do predict FO periods that are systematically longer than observed. Note that the minimum period for FO pulsators based on canonical models agree quite well with observed values in GCs (Caputo et al. 2000; Di Criscienzo, Marconi & Caputo 2004). iii)– Metal-poor (top) and metal-intermediate (bottom) He-enhanced models show the same behavior. iv)– The period range covered by canonical RR Lyrae models agrees quite well with the observed one.

The anonymous referee suggested to provide a more detailed comparison between theory and observations using synthetic HB models. To accomplish this goal we computed a series of synthetic HB using the same theoretical framework adopted by Percival et al. (2009). Note that the main aim of this approach is to constrain the impact that different HB sub-populations characterized by different He contents have on the period distribution of RR Lyrae stars. We adopted two different assumptions concerning the mass distribution to populate the synthetic HBs. In particular, we adopted a linear sampling and a Gaussian

---

[4]The long period tail of RR Lyrae stars in ω Cen includes seven objects with periods ranging from ~0.81 to ~0.87 day and with mean visual magnitudes ranging from 14.32 (V31) to 14.56 (V78) mag. These objects are well separated from Type II Cepheids, since there is a group of six variables with periods ranging from ~0.97 to ~2.27 day and mean visual magnitudes that are at least half magnitude brighter than long period RR Lyrae stars. Their mean visual magnitude range from 13.32 (V134) to 13.98 (V2, Kaluzny et al. 1997). The sample of Type II Cepheids in ω Cen also includes three Type II Cepheids with periods ranging from ~4.27 to 29.35 day (Kaluzny et al. 1997; Matsunaga et al. 2006).
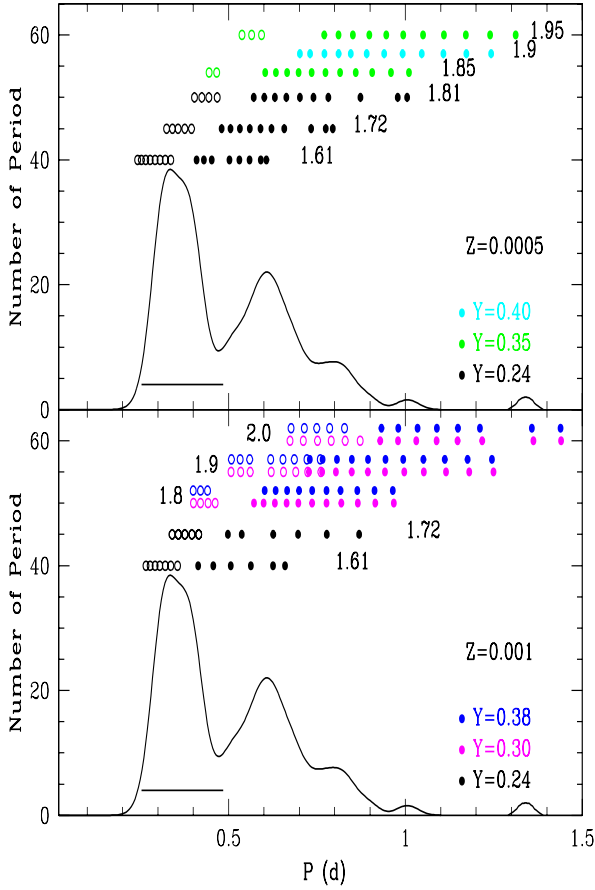
Fig. 3.— Top – Smoothed period of RR Lyrae stars in ω Cen compared with metal-poor ($Z = 0.0005$) predicted periods computed assuming canonical and He-enhanced abundances. The symbols are the same as in Fig. 1. The adopted He abundances and luminosity levels are labelled. The horizontal solid line plotted inside the observed period distribution shows the period range covered by FO RR Lyrae in ω Cen. Bottom – same as the top, but for metal-intermediate structures ($Z = 0.001$).
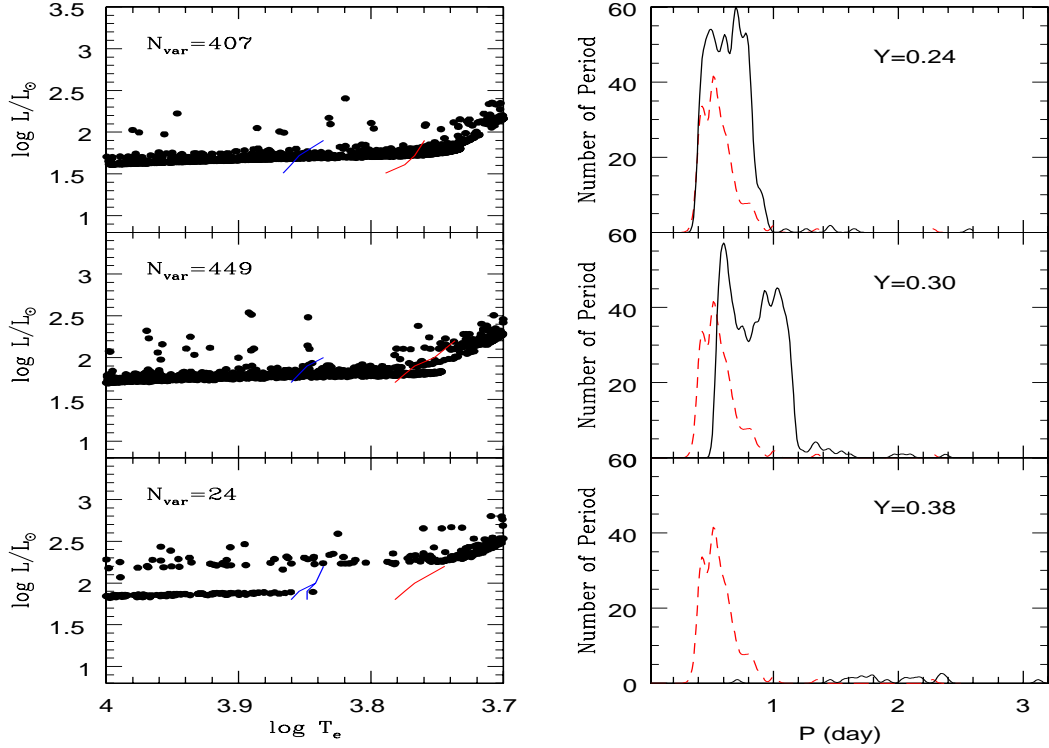
Fig. 4.— Left – Hertzsprung-Russell Diagram showing synthetic HB models constructed assuming a linear sampling in mass. The blue and the red lines display the first overtone blue edge and the fundamental red edge. From top to bottom the three panels display predictions based on HB models with different helium contents: Y=0.24 (top), Y=0.30 (middle) and Y=0.38 (bottom). The number of stars located inside the instability strip are labeled. Right – Comparison between the period distribution of the synthetic HB models (black line) plotted in the left panels and the observed period distribution (red dashed line). The period of the first overtones were fundamentalized ($\log P_F = \log P_{FO} + 0.127$). Predicted and observed period distributions were smoothed using a Gassian kernel.

sampling. In the former case we distributed –for each chemical composition– 4,000 artificial stars according to the evolutionary lifetimes predicted by a detailed grid of HB models. Data plotted in the left panels of Fig. 4 show the synthetic HBs, while the right panels display the period distribution of the objects located between the blue edge of the first overtones and the red edge of the fundamental mode. In the comparison between predicted (solid line) and observed (red dashed line) period distribution, we fundamentalize the period of the first overtones (log P_F=log P_{FO}+0.127). The predicted period distributions were smoothed using the same approach adopted for the observed one. Data plotted in the top right panel indicate that a significant fraction of HB stars populating the warm and the hot region of the HB might have a canonical helium content.

The minimum fundamentalized period is a robust observable to constrain the evolutionary properties of RR Lyrae stars (the interested reader is referred to Bono et al. 1995, and references therein). We found that the observed minimum fundamentalized period is $\sim$ 0.34 day, while the predicted one, assuming a canonical helium abundance is $\sim$ 0.39 day. Moreover, the predicted distribution shows a well defined upper limit for RR Lyrae stars at $P \sim$0.87 day as suggested by the observations. The shape of the predicted period distribution is broader than the observed one, but this difference is out of the aim of this investigation. Note that the predicted fraction of Type II Cepheids with periods 0.95$\leq$P$\leq$2.30 is a factor of three smaller ($\sim$1%) than the observed one ($\sim$3%). Empirical evidence indicates that only six Type II Cepheids with 0.95$\leq$ P $\leq$2.3 have been identified in ω Cen(see Kaluzny et al. 1997).

The synthetic HBs computed assuming the He-enhanced HB models with Y=0.30 show a period distribution that is systematically shifted toward longer periods when compared with the observed one (see the middle right panel of Fig. 4). Moreover, this period distribution shows, at odds with observations, two well separated peaks. The comparison with the period distribution based on HB models with Y=0.38 is more difficult, since these structures do not produce RR Lyrae stars, but only Type II Cepheids. However, the predicted Type II Cepheids attain visual magnitudes that are brighter (V$\leq$13.2$\pm$0.1 mag, see the bottom right panel of Fig. 4) than the observed ones (see Kaluzny et al. 1997). In passing we note that the crossing time of the He-enhanced models, at fixed metal content (Z=0.001), is on average 10% longer (Bono 2010) than for models with canonical He-content. This means that the probability to produce Type II Cepheids for He-enhanced structures is higher than for canonical ones.

The synthetic HB models based on the Gaussian sampling in mass, were constructed adopting for each chemical composition a slightly different value of the mean mass (M/M$_\odot$=0.62 [Y=0.246], 0.61 [Y=0.30], 0.60 [Y=0.38]) populating the HB and the same dispersion in mass
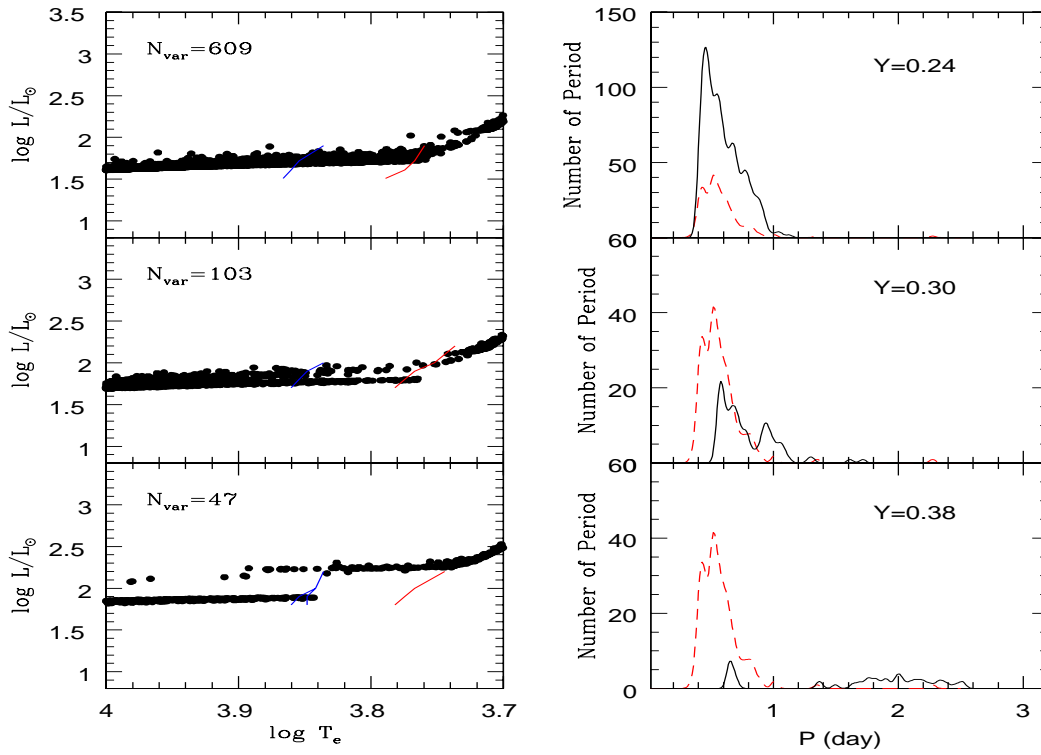
Fig. 5.— Same as Fig. 4, but the synthetic HB models were constructed assuming a Gaussian sampling in mass with different mean masses and the same dispersion. See text for more details.

(σ=0.02 M$_\odot$). Data plotted in Fig. 5 show that the period distribution based on synthetic HB models with Gaussian sampling in mass is very similar to the models with linear sampling. The minimum fundamentalized period of the canonical models is $\sim$ 0.39 day, and the fraction of Type II Cepheids with periods $0.95 \leq P \leq 2.30$ is similar (2%) to the observed one. Moreover, the predicted period distribution shows a well defined peak similar to the observed one. The period distributions based on He-enhanced models show discrepancies similar to synthetic HBs computed assuming a linear sampling in mass.

However, the above conclusions rely on the assumption that warm and hot HB stars are only made by HB structures either with a canonical or with a He-enhanced compositions. Recent investigations concerning the fraction of second generations, He-enhanced stars in GCs indicate that it might be of the order of 50% or even more (D'Antona & Caloi 2008). For ω Cen it was suggested that the fraction of stars with a moderate increase in He content (Y$\leq$ 0.38) should be of the order of 20% (Norris 2004; Lee et al. 2005). To account for the possible mix of RR Lyrae stars with different helium contents Fig. 6 shows the cumulative period distribution computed assuming the 80% of the period distribution based on canonical HB models and the 20% of the period distribution based on helium-enhanced HB models (Y=0.30). Note that we did not apply any normalization between the two period distributions. The cumulative period distribution based on the uniform mass distribution shows a minimum fundamentalized period that is, as expected, very similar to the period distribution based on canonical HB models. However, the fraction of Type II Cepheids with periods $0.95\leq P \leq 2.30$ is almost a factor of three larger (8%) than the observed one. The outcome is similar for the cumulative period distribution based on the Gaussian sampling, but the same fraction is almost a factor of two larger (5%) than the observed one (see the bottom panel of Fig. 6).

The above findings indicate that the fraction of RR Lyrae stars with Y=0.30 cannot be larger than 20%. The occurrence of He-enhanced structures causes a steady increase in the typical period of RR Lyrae stars and an increase in the fraction of Type II Cepheids with periods between 0.95 and 2.30 day that is not supported by observations. These results are minimally affected by the sampling in mass adopted to compute the synthetic HB models. We cannot reach firm conclusions concerning the fraction of HB stars with Y=0.38, since these structures only produce Type II Cepheids. However, the predicted visual magnitudes for these objects are systematically brighter than observed.

To further constrain the impact of the He abundance on the pulsation properties of RR Lyrae stars we also compared observed (Kaluzny et al. 1997) and predicted V-band amplitudes for FU RR Lyrae. Note that luminosity amplitudes are also independent of cluster distance and reddening corrections. Bolometric light curves were transformed into the obser-
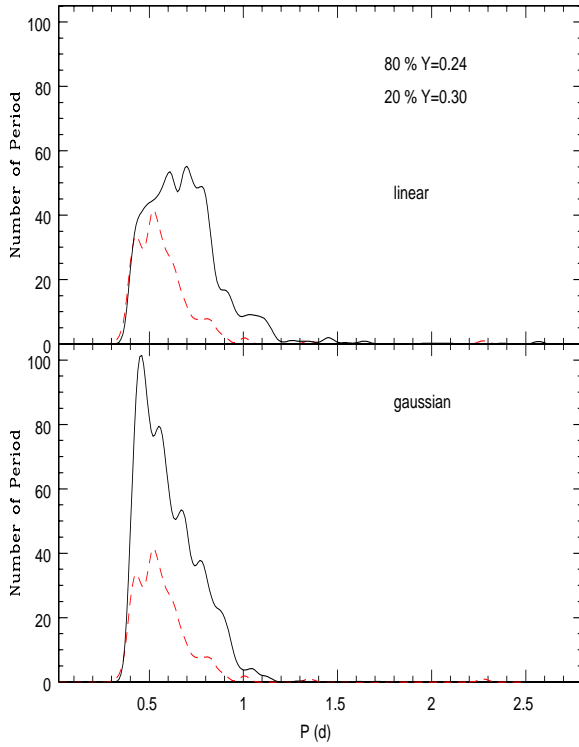
Fig. 6.— Top – Comparison between the observed period distribution and the predicted cumulative period distribution based on the linear sampling in mass (see Fig. 4). The latter was estimated assuming the 80% of the canonical and the 20% of the helium-enhanced (Y=0.30) period distribution. Bottom – Same as the top, but the predicted cumulative distribution is based on the Gaussian sampling in mass (see Fig. 5).
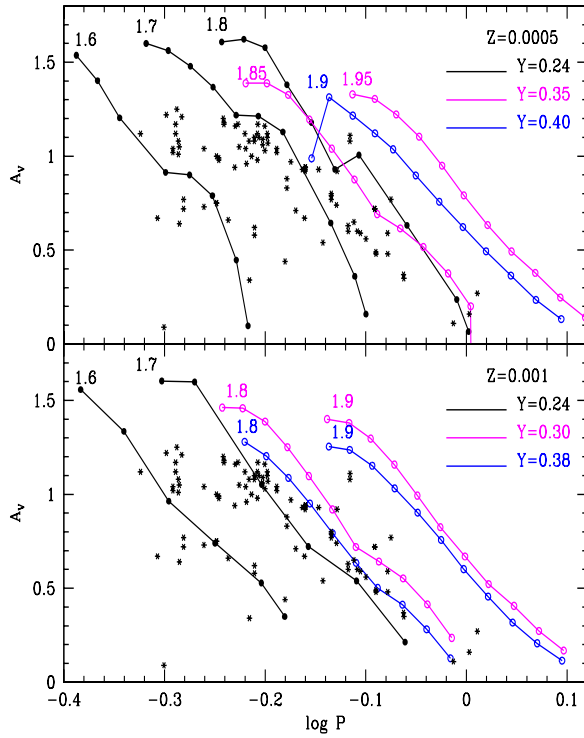
Fig. 7.— Top – Comparison between observed (Kaluzny et al. 1997) and predicted V-band amplitudes versus the logarithmic period for metal-poor ($Z = 0.0005$) RR Lyrae models. The adopted He abundances and luminosity levels are labelled. Bottom – Same as the top, but for metal-intermediate ($Z = 0.001$) RR Lyrae models.

vational plane using the bolometric corrections and the Color-Temperature transformations provided by (Castelli, Gratton & Kurucz 1997a,b). Fig. 7 shows the comparison between observed and predicted V-band amplitudes for canonical (black lines) and He-enhanced (colored lines) RR Lyrae models. Data plotted in this figure indicate, once again, that the He content marginally affects the pulsation behavior of RR Lyrae. The top panel shows that the set of metal-poor models with an increase of 50% in He, when compared with canonical models and with similar luminosities ($\log L/L_\odot \approx$1.85 vs 1.80), display very similar amplitudes and cover very similar periods. The same outcome applies to the two sets of He-enhanced, metal-intermediate RR Lyrae models (bottom panel).

Data plotted in this figure indicate that He-enhanced models only account for the upper envelope of the observed distribution. An increase either in the luminosity level or in the He content increases the discrepancy between theory and observations. The canonical RR Lyrae models are in fair agreement with observations. However, in dealing with luminosity amplitudes we need to keep in mind two limits. *i)*– The theoretical Bailey diagram is affected by uncertainties on the mixing length parameter (see e.g. Marconi et al. 2003).Current pulsation models were constructed by assuming a mixing length parameter $\alpha = 1.5$. In the mixing length formalism, a larger α value means larger efficiency of convective motions, and in turn, smaller pulsation amplitudes. However, we have verified (Marconi et al. 2011, in preparation) that by increasing the mixing length parameter from 1.5 to 2.0, the He-enhanced models do not fit the distribution of the observed amplitudes. Several numerical experiments performed using our theoretical framework show that smaller α values, as the ones recently suggested by asteroseismological results(Piau et al. 2011, and references therein), would predict pulsation observables for RR Lyrae variables that are at odds with observations. This outcome applies not only to the Bailey diagram, but also to the modal stability and the topology of the instability strip. *ii)*– Recent space (COROT, Chadid et al. 2010) and ground-based (Kunder, Chaboyer, & Layden 2010) observations indicate that the fraction of RR Lyrae stars affected by the Blazkho phenomenon is higher than previously estimated ($\approx$50%, Benko et al. (2010). This effect causes a modulation of both amplitudes and phase and unfortunately, we still lack a complete census of Blazkho RR Lyrae in ω Cen.

4. Conclusions and final remarks

To constrain the possible occurrence of He-enriched RR Lyrae stars we adopted two observables –periods, V-band amplitudes– that are independent of cluster distance and reddening. The comparison between theory and observations indicates that the predicted periods and amplitudes of RR Lyrae stars are marginally affected by the He content. The key param-

eter causing the difference between canonical and He-enhanced observables is the luminosity. We found that the period range of He-enhanced RR Lyrae models is systematically longer than observed. These findings apply to metal-poor and metal-intermediate He-enhanced models. The results are the same if we take into account the luminosity amplitude. However, predicted amplitudes are less robust than the pulsation periods, since they depend on the adopted mixing length parameter. Moreover, the amplitude might also be affected by an observational bias, since we still lack a complete census of ω Cen RR Lyrae affected by the Blazkho phenomenon.

Taken at face value the above results indicate that ω Cen RR Lyrae do not show a clear evidence of He-enrichment when moving from metal-poor to metal-intermediate stars. However we cannot exclude, as originally suggested by Sollima et al. (2006), the probable occurrence of two metal-intermediate sub-populations. The former one with canonical He content evolving into the RR Lyrae IS and the latter one with a He-enhanced abundance evolving into the hot and the EHB region. Note that ω Cen hosts more than 2,100 hot HB stars, i.e. roughly the 65% of the entire population of HB stars (see Table 2 in Castellani et al. 2007).

To constrain the occurrence of He-enhanced RR Lyrae stars we also computed a series of synthetic HB models using canonical and He-enhanced HB models and two different assumptions concerning the sampling in mass (linear, Gaussian). Current models further confirm the sensitivity of the minimum fundamentalized period to constrain the He content of cluster RR Lyrae. The period distribution based on canonical HB models agree quite well with observations concerning the minimum period (0.39 vs 0.34), the upper limit to the period distribution of RR Lyrae stars (P$\sim$0.87 day) and the fraction (2% vs 3 %) of Type II Cepheids (0.95$\leq$P$\leq$2.30 day). These findings minimally depend on the adopted sampling in mass.

The period distribution based on He-enhanced HB models is either systematically shifted towards longer periods (Y=0.30) or produce Type II Cepheids that are systematically brighter than observed (Y=0.38). To further constrain the impact on the period distribution of RR Lyrae with different He contents we computed the period distribution of a sample made with the 80% of canonical and the 20% of RR Lyrae stars with moderate He-enhancement (Y=0.30). We found that the fraction of Type II Cepheids predicted by the synthetic HB models computed by assuming a Gaussian sampling in mass is almost a factor of two larger than observed (5% vs 3%). This indicates that the fraction of He-enhanced structures in ω Cen cannot be larger than 20%.

More quantitative constraints concerning the individual He abundances of RR Lyrae

stars in ω Cen requires accurate estimates of the A-parameter[5] (Caputo et al. 1983; Sandquist 2000) using homogeneous grids of pulsation and evolutionary models constructed assuming a broad range of helium abundances (Caputo et al. 2011, in preparation).

Finally, in a recent investigation (Dupree, Strader & Smith 2011) detected in five out of twelve RGs in ω Cen, with similar magnitudes and colors, the chromospheric HeI line at 10830Å. The strength of the He line seems to be correlated with Al and Na abundances rather than with iron. However, a more detailed non-LTE analysis of the He abundance is required before firm conclusions concerning the occurrence of a spread in helium can be safely established.

REFERENCES

Alexander, D. R., Ferguson, J. W. 1994, ApJ, 437, 879

Anderson, J. 2002, ASPC, 265, 87

Bedin, L. R. et al. 2004, ApJ, 605, 125

Bellini, A., Bedin, L. R., Piotto, G., Milone, A. P., Marino, A. F., Villanova, S. 2010, AJ, 140, 631

Benko, J. M., Kolenberg, K., Szabó, R. et al. 2010, MNRAS, 409, 1585

Bergbusch, P. A., Stetson, P. B. 2009, AJ, 138, 1455

Bono, G. 2010, MmSAI, 81, 863

Bono, G., Marconi, M., Stellingwerf, R.F. 1999, ApJS, 122, 167

---

[5]The A-parameter is a diagnostic to constrain the mass-luminosity ratio of individual RR Lyrae stars. It is defined as: A= $\log L/L_\odot - 0.81 \log M/M_\odot$, where L and M are the luminosity and the mass of the pulsator.

Bono, G., Caputo, F., Castellani, V., Marconi, M. 1995, ApJ, 448, 115

Bono, G., Caputo, F., Castellani, V., Marconi, M., Storm, J., Degl'Innocenti, S. 2003, MNRAS, 344, 1097

Bono, G., Stetson, P. B., Sanna, N. et al. 2008, ApJ, 686, 87

Bono, G., Stellingwerf, R.F. 1994, ApJS, 93, 233

Brown, T. M., Sweigart, A. V., Lanz, T., Smith, E. et al. 2010, ApJ, 718, 1332

Calamida, A., Bono, G., Stetson, P. B. et al. 2007, ApJ, 670, 400

Calamida, A., Bono, G., Stetson, P. B. et al. 2009, ApJ, 706, 1277

Caputo F., Cayrel R., Cayrel de Strobel G., 1983, A&A, 123, 135

Caputo, F., Castellani, V., Marconi, M., Ripepi, V. 2000, MNRAS, 316, 819

Cassisi, S., Salaris, M., Pietrinferni, A. et al. 2008, ApJ, 672,L115

Cassisi, S., Salaris, M., Anderson, J., et al. 2009, ApJ, 702, 1530

Castellani, V., Calamida, A., Bono, G. et al. 2007, ApJ, 663, 1021

Castelli, F., Gratton, R. G., & Kurucz, R. L. 1997a, A&A, 318, 841

Castelli, F., Gratton, R. G., & Kurucz, R. L. 1997b, A&A, 324, 432

Chadid, M., Benko, J. M., Szabó, R. et al. 2010, A&A, 510, 39

D'Antona, F., Caloi, V., Ventura, P. 2010, MNRAS, 405, 2295

D'Antona, F. & Caloi, V. 2008, MNRAS, 390, 693

Del Principe et al. 2006, ApJ, 652, 362

Di Cecco, A., Bono, G., Stetson, P. B. et al. 2010, ApJ, 712, 527

Di Criscienzo, M., Marconi, M., Caputo, F. 2004, ApJ, 612, 1092

Di Criscienzo, M., Ventura, P., D'Antona, F., Milone, A., & Piotto, G. 2010, MNRAS, 408, 999

Dupree, A. K., Strader, J., Smith, G. H. 2011, ApJ, 728, 155

Gratton, R., Sneden, C., & Carretta, E. 2004, A&A, 42, 385

Iglesias, C., Rogers, F. J. 1996, ApJ, 464, 943

Kaluzny, J., Kubiak, M., Szymanski, M., Udalski, A., Krzeminski, W., Mateo, M. 1997, A&AS, 125, 343

Kaluzny, J., Olech, A., Thompson, I. B., Pych, W., Krzemiński, W., Schwarzenberg-Czerny, A. 2004, A&A, 424, 1101

Kraft, R. P. 1994, PASP, 106, 553

Kunder, A., Chaboyer, B., Layden, A. 2010, AJ, 139, 415

Lee, Y.-W., Joo, S.-J., Han, S.-I. et al. 2005, ApJ, 621, 57

Lee, J.-W., Kang, Y.-W., Lee, J., Lee, Y.-W. 2009b, Nature, 462, 480

Marconi, M., Caputo, F., Di Criscienzo, M., Castellani, M. 2003, ApJ, 596, 299

Miller Bertolami, M. M., Althaus, L. G., Unglaub, K., & Weiss, A. 2008, A&A, 491, 253

Milone, A. P., Bedin, L. R., Piotto, G. et al. 2008, ApJ, 673, 241

Moehler, S. Dreizler, S., Lanz, T., Bono, G., Sweigart, A. V., Calamida, A., Nonino, M. 2011, A&A, 526, 136

Nataf, D. M., Gould, A., Pinsonneault, M. H., Stetson, P. B. 2011, submitted ApJ, arXiv1102.3916

Norris, J. E. 2004, ApJ, 612, 25

Osborn, W. 1971, The Observatory, 91, 223

Piau, L., Kervella, P., Dib, S., Hauschildt, P. 2011, A&A, 526, 100

Pietrinferni, A., Cassisi, S., Salaris, M., Castelli, F. 2006, ApJ, 642, 797

Pilachowski, C. A., Sneden, C., & Wallerstein, G. 1983, APJS, 52, 241

Piotto, G. et al. 2005, ApJ, 621, 777

Piotto, G. et al. 2007, ApJ, 661, 53

Sandquist, E. L. 2000, MNRAS, 313, 571

Smith, G. H. 1987, PASP, 99, 67l

Sollima, A. et al. 2006, ApJ, 640, 43

Smolec, R., Moskalik, P. 2010, A&A, 524, 40

Siegel, M. H., et al. 2007, ApJ, 667, L57

Stellingwerf, R. F. 1982, ApJ, 262, 330

Weldrake, David T. F., Sackett, Penny D., Bridges, Terry J. 2007, AJ, 133, 1447